

Supporting Information

Liquid Gallium Nanospheres Emitting White Light

Jin Xiang^{1*}, Jingdong Chen^{1*}, Shuai Jiang¹, Mingcheng Panmai¹, Peilian Li², Yi Xu³, Qiaofeng Dai¹, Shaolong Tie⁴, and Sheng Lan^{1*}

Dr. Jin Xiang, Jingdong Chen, Shuai Jiang, Mingcheng Panmai, Qiaofeng Dai, Prof. Sheng Lan,

Guangdong Provincial Key Laboratory of Nanophotonic Functional Materials and Devices
School of Information and Optoelectronic Science and Engineering

South China Normal University

Guangzhou, 510006, P. R. China

slan@scnu.edu.cn (S. Lan)

Dr. Peilian Li

Institute for Advanced Materials and Guangdong Provincial Key Laboratory of Quantum Engineering and Quantum Materials, South China Academy of Advanced Optoelectronics, South China Normal University, Guangzhou 510006, China

Prof. Yi Xu

Department of Electronic Engineering

College of Information Science and Technology

Jinan University

Guangzhou, 510632, P. R. China

Prof. Shaolong Tie

School of Chemistry and Environment

South China Normal University

Guangzhou, 510006, P. R. China

S1: Scattering properties of Ga nanospheres

The scattering spectra of Ga nanospheres (NSs) can be calculated by using Mie theory^{1,2}. In Figure S1a, we show the scattering spectrum calculated for a Ga NS with a diameter (d) of 240 nm. The contributions of electric dipole (ED), quadrupole (EQ) and octapole (EOC) to the total scattering are also presented. In order to see the evolutions of the ED, EQ and EOC modes with increasing diameter of the Ga NS, we calculated the evolution of the total scattering spectrum with increasing diameter from 80 to 280 nm, as shown in Figure S1b. As compared with the EQ and EOC resonances, a larger redshift of the ED resonance is observed. In practice, one can only characterize the forward or backward scattering properties of nanoparticles. In Figure S1c, we show the evolution of the forward scattering spectrum with increasing diameter of the Ga NS. It is noticed that the scattering intensity at the resonant wavelength of the EQ mode is much stronger than that of the ED mode. The underlying physical mechanism for this phenomenon is the coherent interaction between the EQ and ED modes. In Figure S1d, we present the two-dimensional radiation patterns of the Ga NS calculated at 750 and 400 nm, which correspond to the resonant wavelengths of the ED and EQ modes, respectively. At 750 nm, the radiation is caused by a nearly pure ED mode. In this case, the forward and backward scattering intensities are almost equal. In sharp contrast, a highly directional scattering in the forward direction is observed at 400 nm where a strong coupling between the EQ and ED modes is expected. The constructive interference between the EQ and ED modes in the forward direction and the destructive interference in the backward direction are responsible for the highly directional scattering observed at 400 nm.

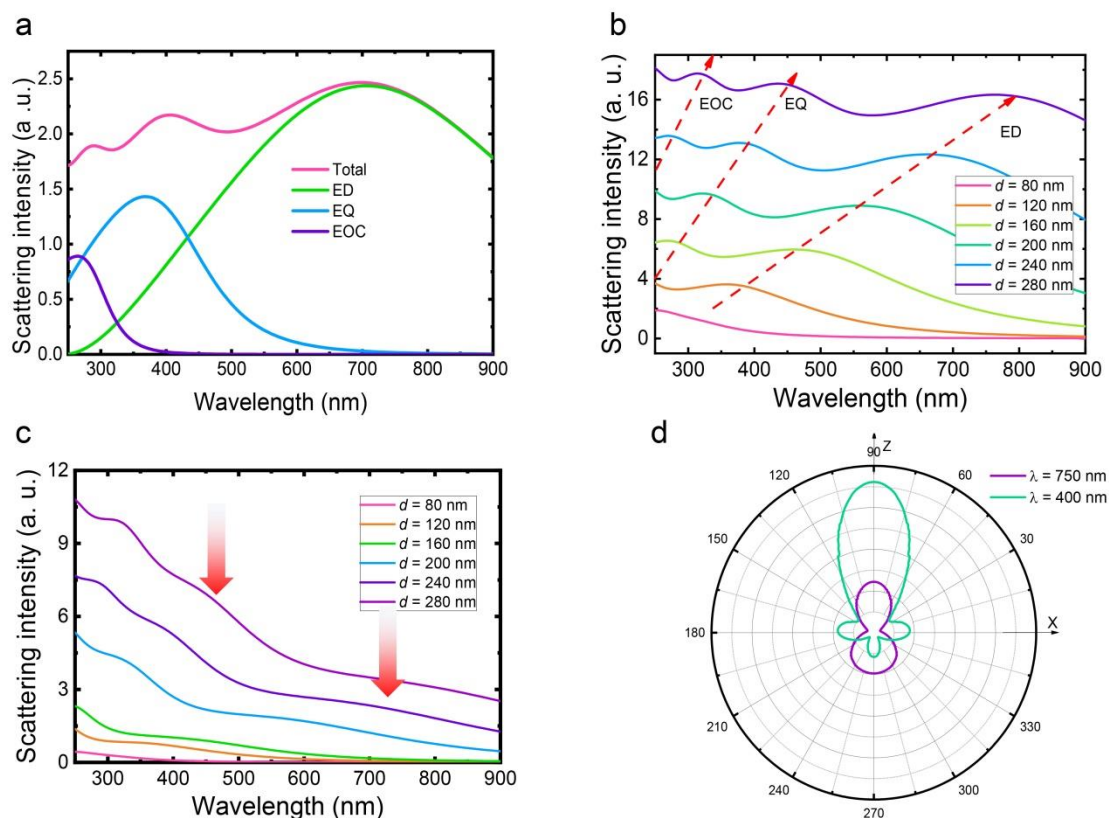
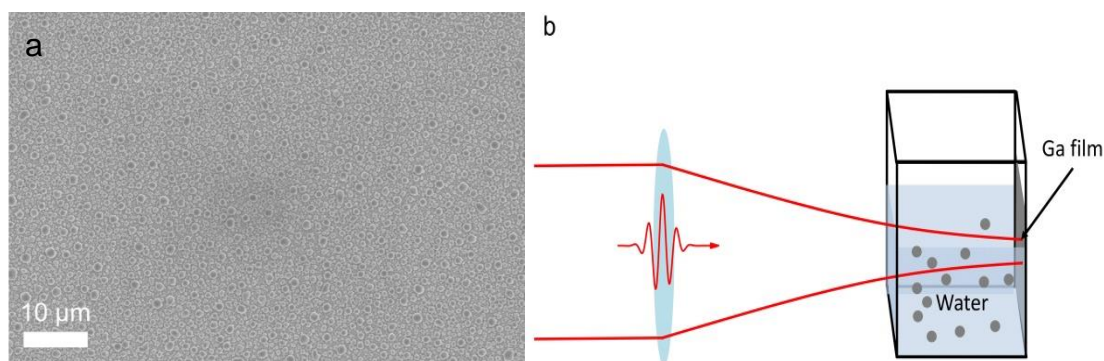


Figure S1. Scattering properties of Ga NSs. (a) Scattering spectrum calculated for a Ga NS with $d = 240$ nm based on Mie theory. The total scattering has been decomposed into the contributions of ED, EQ and EOC modes. (b) Evolution of the total scattering spectrum of a Ga NS with increasing diameter simulated by using the FDTD method. (c) Evolution of the forward scattering spectrum of a Ga NS with increasing diameter simulated by using the FDTD method. (d) Two-dimensional radiation patterns calculated for a Ga NS with $d = 240$ nm at 400 and 750 nm.

S2: Fabrication of Ga nanospheres by using femtosecond laser ablation

The material target used in the femtosecond laser ablation was a Ga film prepared by using thermal evaporation. The surface of the Ga film was examined by scanning electron microscopy (SEM) observation, as shown in Figure S2a. In the fabrication of Ga NSs, the Ga film was placed on the back wall of a glass vessel which was filled with water. The femtosecond laser light was focused on the surface of the Ga film by using a 25-cm focusing length objective, as schematically shown in Figure S2b. The diameter of the laser beam was estimated to be ~ 40 μm . The scattering properties of the fabricated Ga NSs were examined by using conventional dark-field microscopy. The radiation patterns of the Ga NSs recorded by using a charge coupled devices are shown in Figure S2c.



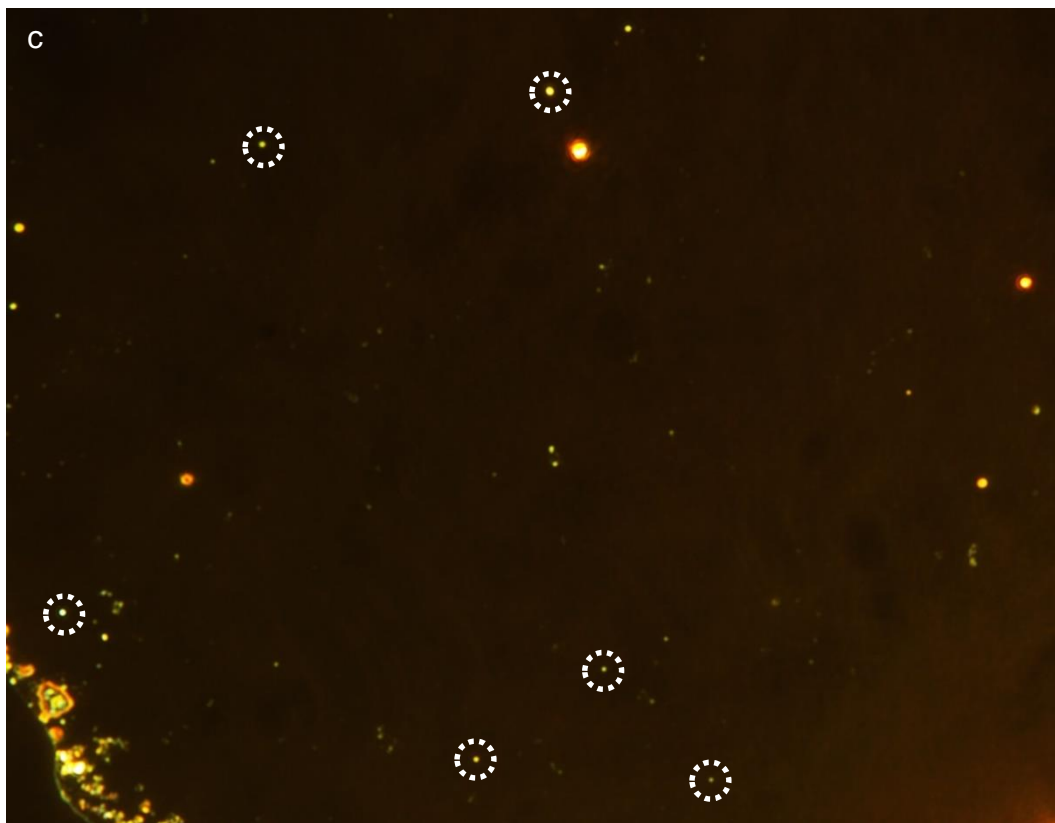


Figure S2. (a) SEM image of the Ga film used for the fabrication of Ga nanospheres. (b) Schematic showing the experimental setup used to fabricate Ga nanospheres in water. (c) CCD images of the fabricated Ga nanospheres under a dark-field microscope.

S3: Experimental setup used to characterize the nonlinear optical responses of Ga nanospheres

In Figure S6, we show schematically the experimental setup used to characterize the nonlinear optical responses of Ga NSs. The femtosecond laser light from a Ti : sapphire oscillator was introduced into an inverted microscope, reflected by a dichroic mirror and focused on the Ga NS by using the 100 \times objective of the microscope. The nonlinear optical signals generated by the Ga NS were collected by using the same objective and directed to a spectrometer for analysis. A stop-band filter with a narrow bandwidth of ~ 40 nm was inserted in the collection channel to remove the reflected excitation laser light.

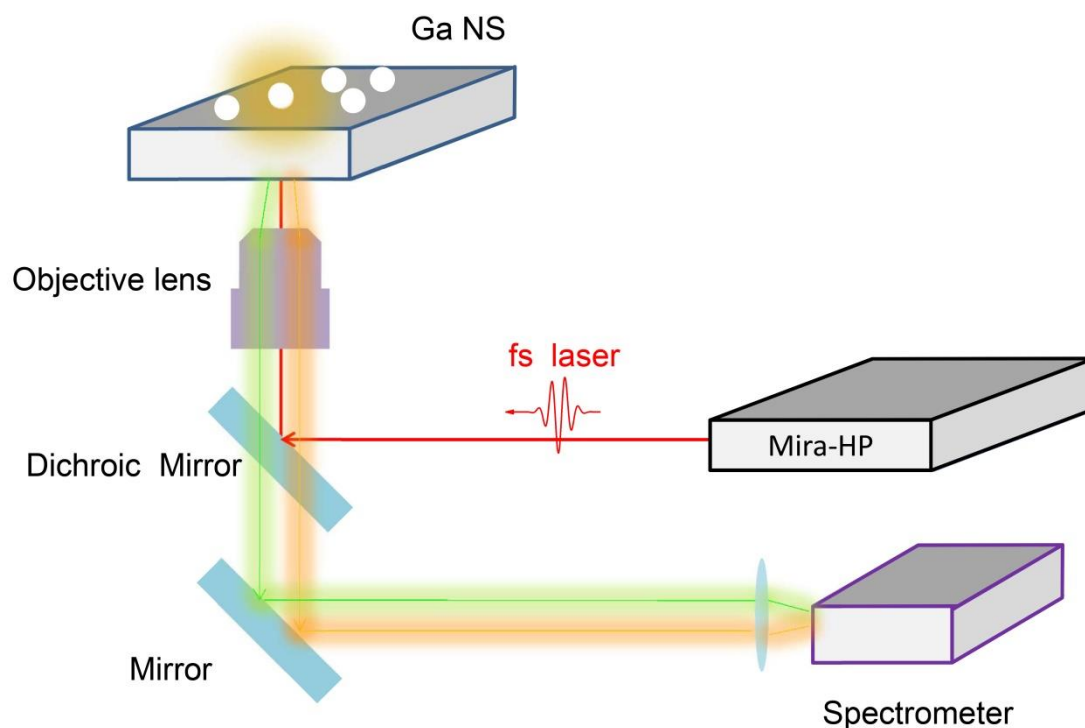


Figure S3. Schematic showing the experimental setup used to characterize the nonlinear optical responses of Ga NSs.

S4: Complex dielectric constants of solid and liquid Ga

In previous literature, there is very few data for the complex dielectric constants of solid and liquid Ga. In order to simulate the scattering properties of Ga NSs, an accurate data for the complex dielectric constants of Ga in solid and liquid phases is quite important. In this work, we used the complex dielectric constants reported in the following (Refs. 3 and 4) in the numerical simulations, as shown in Figure S7.

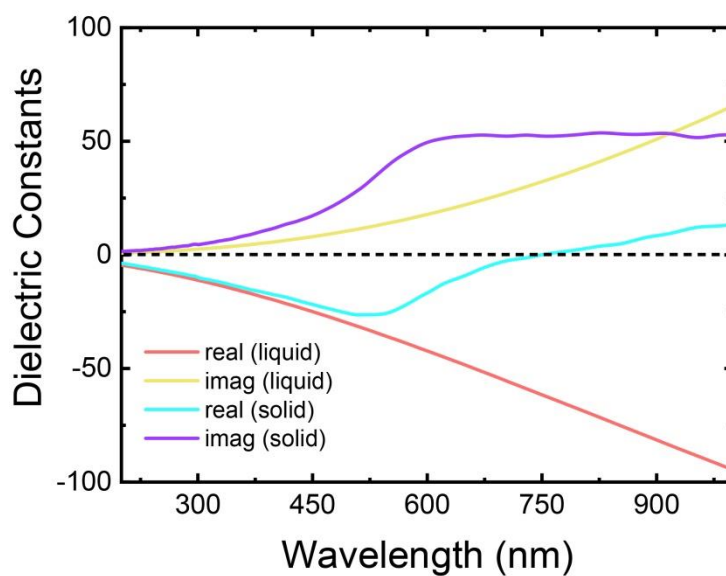


Figure S4. Complex dielectric constants of solid and liquid Ga. Wavelength dependence of the real and imaginary parts of the complex refractive indices for solid and liquid Ga used in the calculation of the scattering spectra of Ga nanospheres.

S5: Backward scattering spectra of Ga nanospheres and electric field enhancements

We calculated the scattering spectra of a Ga NS with $d = 240$ nm illuminated by s - and p -polarized light, as shown in Figure S3a and S3b. In each case, a Fano dip is clearly observed in the scattering spectrum. In order to confirm that the scattering valley is actually a Fano resonance, we also calculated the spectra of $[\int |E(\lambda)|^4 dV]/V$ and $[\int |E(\lambda)|^6 dV]/V$, which represent the two- and three-photon-induced absorption of nanoparticles upon the excitation of femtosecond laser pulses. It can be seen that the maxima of both $[\int |E(\lambda)|^4 dV]/V$ and $[\int |E(\lambda)|^6 dV]/V$ indeed appear at the scattering valley, verifying that the scattering valley is actually a Fano dip with significantly enhanced electric field.

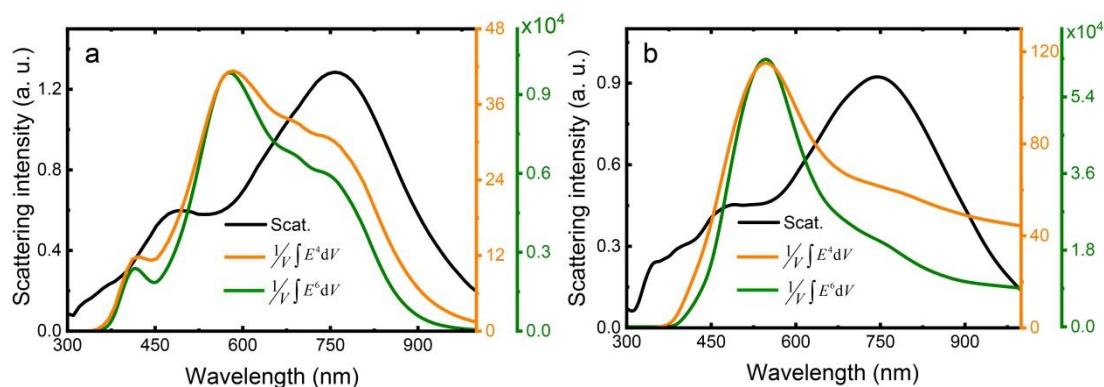


Figure S5. Scattering and electric field enhancement spectra of Ga NSs. Backward scattering spectra calculated for a Ga NS with $d = 240$ nm illuminated by (a) s - and (b) p -polarized light at an incidence angle of 36° . The corresponding electric field enhancement spectra calculated for the Ga NS are also provided.

S6: Scattering properties of Ga nanospheres placed on a glass substrate

We measured the forward and backward scattering spectra of Ga NSs placed on a glass substrate. A typical example is shown in Figure S4a. It can be seen that the spectral shapes in the forward and backward directions are much different. While the forward scattering spectrum is dominated by the coherent interaction between the EQ and ED modes, the backward scattering spectrum is governed by the radiation of the ED mode. In Figure S4b, we show the calculated spectra in the forward and backward directions. Considering the significantly reduced quantum efficiency of the spectrometer in the ultraviolet spectral region, the measured spectra are in good agreement with the simulated ones.

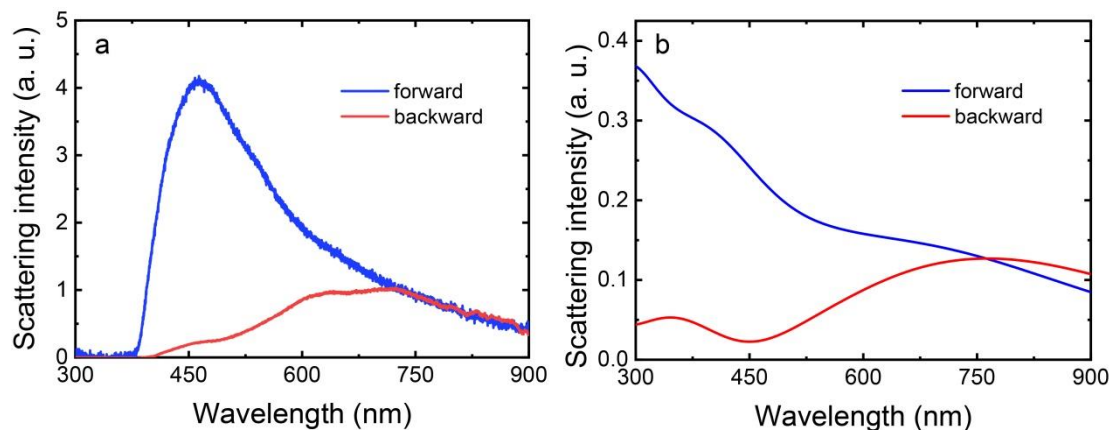


Figure S6. Scattering properties of Ga NSs placed on a glass substrate. (a) Forward and backward scattering spectra measured (a) and calculated (b) for a Ga NS with $d \sim 240$ nm.

S7: Hot-electron intraband luminescence from Ga nanospheres

Hot-electron intraband luminescence, which is quite similar to blackbody radiation, has been recently observed in single plasmonic hot spots and semiconductor nanoparticles. In order to identify the nature of the photoluminescence from Ga NSs, we have performed spectral analysis for Ga NSs excited by using femtosecond laser pulses with different excitation irradiances. A typical example is shown in Figure S5 where the relationship between the slope extracted from the dependence of the luminescence intensity on the excitation irradiance and the energy of the emitted photon is presented. In both the low and high excitation irradiance regimes, a linear relationship between the slope and the energy of the emitted photon is observed. In the high excitation irradiance regime, the straight line can be extrapolated to the origin of the coordinate. This is a unique feature of hot-electron intraband luminescence, imply that the photoluminescence from Ga NSs in the high excitation irradiance regime is actually hot-electron intraband luminescence. In comparison, a smaller slope is observed in the low excitation irradiance regime, as shown in Figure S5.

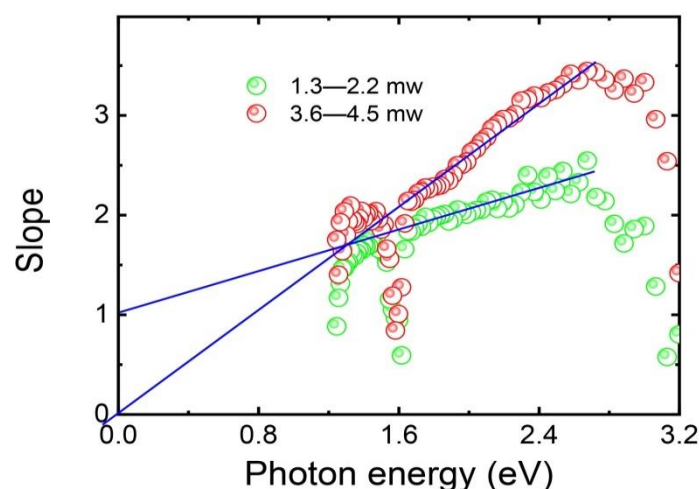


Figure S7. Hot-electron intraband luminescence from a Ga NS. Relationships between the slope extracted from the dependence of the luminescence intensity on the excitation irradiance and the energy of the emitted photon measured in the low (green symbols) and high (red symbols) excitation irradiance regimes.

S8: Dependence of the luminescence intensity on the size of the Ga nanosphere

In Figure S8, we present the dependence of the luminescence intensity on the size of the Ga NS, which determines the localization of the Fano dip. In Figure S8a, one can see a redshift of the Fano dip with increasing the diameter of the Ga NS. In experiments, we fixed the excitation wavelength of the fs laser light at 650 nm and measured the hot-electron intraband luminescence spectra for Ga NSs with diameters, as shown in Figure S6b. It is noticed that the strongest luminescence was observed in the Ga NS with $d \sim 280$ nm, as shown in Figure S6c. In this case, the Fano dip formed in the scattering spectrum of the Ga NS coincides with the excitation wavelength of the fs laser light.

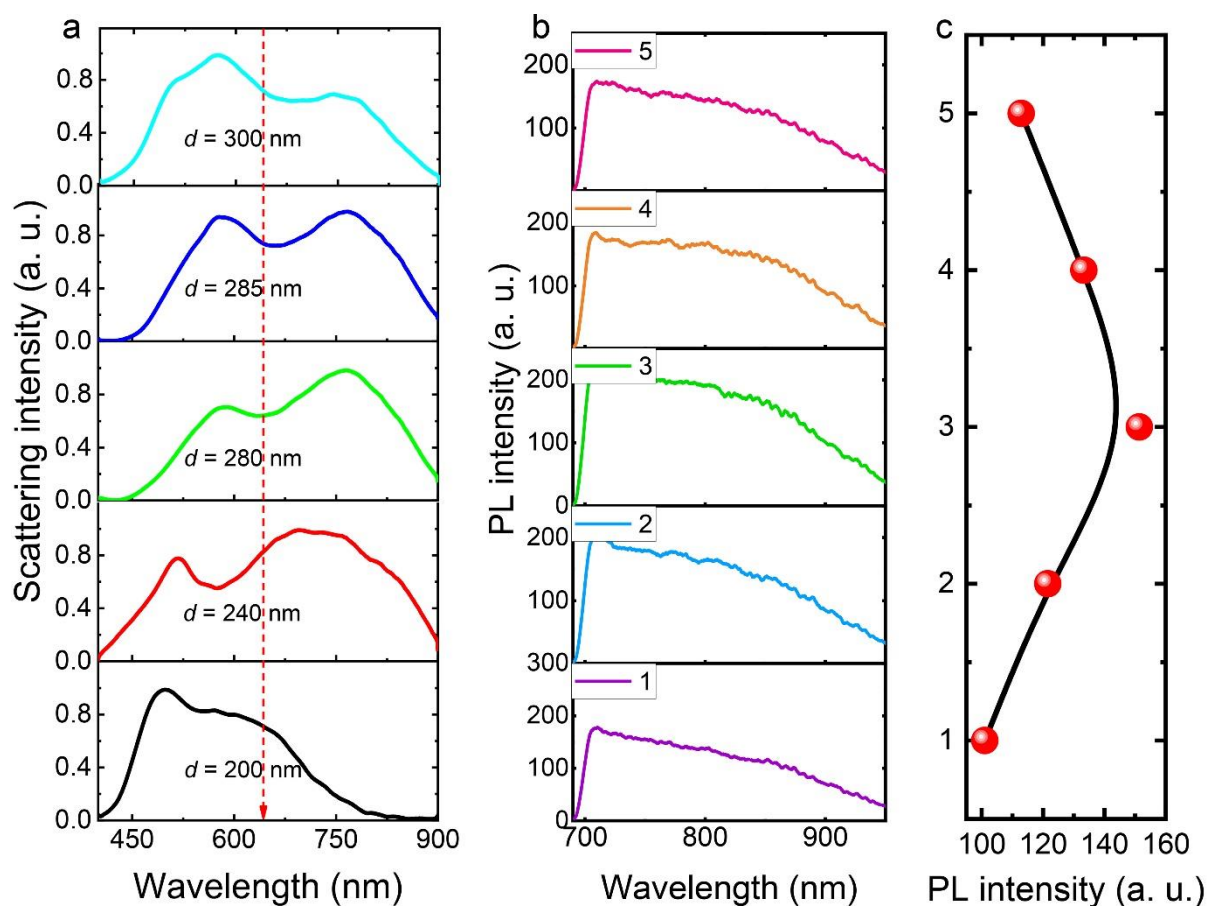


Figure S8. (a) Scattering spectra of Ga NSs with different diameters. (b) Hot-electron intraband luminescence spectra measured for the GNs whose scattering spectra are shown in (a). The excitation wavelength of the fs laser light was chosen at 650 nm, as indicated by the dashed line in (a). (c) Dependence of the luminescence intensity on the size of the Ga NS, which determines the location of the Fano dip.

References

1. Xiang, J.; Li, J.; Li, H.; Zhang, C.; Dai, Q.; Tie, S.; Lan, S. *Opt. Express* **2016**, *24*, 11420-11434.
2. Kuznetsov, A. I.; Miroshnichenko, A. E.; Fu, Y. H.; Viswanathan, V.; Rahmani, M.; Valuckas, V.; Pan, Z. Y.; Kivshar, Y.; Pickard, D. S.; Luk'yanchuk, B. *Nat. Commun.* **2014**, *5*, 3104.
3. Knight, M. W.; Coenen, T.; Yang, Y.; Brenny, B. J. M.; Losurdo, M.; Brown, A. S.; Everitt, H. O.; Polman, A. *ACS Nano* **2015**, *9*, 2049-2060.
4. Kim, S.; Kim, J.-M.; Park, J.-E.; Nam, J.-M. *Adv. Mater.* **2018**, 1704528.